The Plant Cell, Vol. 23: 2606–2618, July 2011, www.plantcell.org

Augmin Plays a Critical Role in Organizing the Spindle and Phragmoplast Microtubule Arrays in *Arabidopsis* [W]

Chin-Min Kimmy Ho,[a,1] Takashi Hotta,[a,1] Zhaosheng Kong,[a,1] Cui Jing Tracy Zeng,[a,1] Jie Sun,[a,b] Yuh-Ru Julie Lee,[a] and Bo Liu[a,2]

[a] Department of Plant Biology, University of California, Davis, California 95616
[b] College of Agriculture, Shihezi University, Shihezi, Xinjiang 832003, China

In higher plant cells, microtubules (MTs) are nucleated and organized in a centrosome-independent manner. It is unclear whether augmin-dependent mechanisms underlie spindle MT organization in plant cells as they do in animal cells. When *AUGMIN subunit3* (*AUG3*), which encodes a homolog of animal dim γ-tubulin 3/human augmin-like complex, subunit 3, was disrupted in *Arabidopsis thaliana*, gametogenesis frequently failed due to defects in cell division. Compared with the control microspores, which formed bipolar spindles at the cell periphery, the mutant cells often formed peripheral half spindles that only attached to condensed chromosomes or formed elongated spindles with unfocused interior poles. In addition, defective cells exhibited disorganized phragmoplast MT arrays, which caused aborted cytokinesis. The resulting pollen grains were either shrunken or contained two nuclei in an undivided cytoplasm. AUG3 was localized along MTs in the spindle and phragmoplast, and its signal was pronounced in anaphase spindle poles. An AUG3-green fluorescent protein fusion exhibited a dynamic distribution pattern, similar to that of the γ-tubulin complex protein2. When AUG3 was enriched from seedlings by affinity chromatography, AUG1 was detected by immunoblotting, suggesting an augmin-like complex was present in vivo. We conclude that augmin plays a critical role in MT organization during plant cell division.

INTRODUCTION

In higher plant cells, microtubules (MTs) are organized into distinct arrays in the absence of structurally defined MT-organizing centers like the spindle pole body of fungi and the centrosome of animals. As a consequence, mitotic spindles exhibit incompletely focused poles and sometimes even assume a barrel-like appearance (Palevitz, 1993). Two distinct pathways lead to the formation of the bipolar spindle in the absence of the centrosome (Lloyd and Chan, 2006). In most dividing somatic cells, prior to nuclear envelope breakdown, MTs surrounding the nucleus are organized into a prophase spindle array with distinct polar caps. In such cases, the establishment of the bipolar prophase spindle depends on the preprophase band (Ambrose and Cyr, 2008). Alternatively, in some plant cells, MTs nucleate around the chromosomes after nuclear envelope breakdown. These randomly oriented MTs are then organized into the bipolar spindle array. Similarly, in acentriolar animal cells, the chromosome-based spindle assembly process is also observed and known to be dependent on MT motors (Karsenti and Vernos, 2001). To date, very little has been learned about proteins that regulate spindle assembly in plant cells.

A key event during spindle assembly is the rapid generation of new MTs in an organized fashion. This process would depend on various factors acting on MTs in a spatially and temporally regulated manner. Among them, γ-tubulin and its associated proteins form the γ-tubulin ring complex to act at MT-organizing centers and are essential for MT nucleation and organization (Job et al., 2003; Wiese and Zheng, 2006). In plant cells, γ-tubulin is associated with spindle and phragmoplast MT arrays with biases toward MT minus ends (Liu et al., 1993). The association of γ-tubulin with spindle MTs in addition to the centrosome is now a recognized fact in animal cells (Lüders and Stearns, 2007). This localization pattern poses the question of whether γ-tubulin interacts with the surface of MTs or the MT wall in the spindle and phragmoplast.

In plant cells, γ-tubulin–dependent MT nucleation on extant MTs is likely the basis of generating nascent MT branches (Murata et al., 2005). In interphase plant cells, MTs generated on existing MTs assume angles of ~40° (Murata et al., 2005, 2007). The branching angle is directly influenced by the γ-tubulin complex (Nakamura and Hashimoto, 2009; Kong et al., 2010). Due to technical challenges, such a phenomenon has not been observed inside the spindle or phragmoplast in living cells so that it is unclear whether these mitotic arrays exercise a similar mechanism to propagate MTs. Interestingly, the concept of MT-dependent MT nucleation is now implicated in generating new MTs in spindles in animal cells (Goshima and Kimura, 2010). Unfortunately, it is still unknown how the interaction between the γ-tubulin complex and the surface of MTs of either the cortical or mitotic arrays is established.

An RNA interference–based screen for proteins required for γ-tubulin localization and consequently for mitotic spindle assembly has revealed an eight-subunit augmin complex in the fly *Drosophila melanogaster* (Goshima et al., 2007, 2008). A similar

[1] These authors contributed equally to this work.
[2] Address correspondence to bliu@ucdavis.edu.
The authors responsible for distribution of materials integral to the findings presented in this article in accordance with the policy described in the Instructions for Authors (www.plantcell.org) are: Yuh-Ru Julie Lee (yjlee@ucdavis.edu) and Bo Liu (bliu@ucdavis.edu).
[W] Online version contains Web-only data.
www.plantcell.org/cgi/doi/10.1105/tpc.111.086892

complex has been isolated from human cells for its role in centrosome-independent MT generation in spindles and chromosome segregation (Lawo et al., 2009; Uehara et al., 2009; Hutchins et al., 2010). Augmin and the γ-tubulin complex appear to interact via the WD40 repeat protein NEDD1/GCP-WD (Zhu et al., 2008; Uehara et al., 2009). Among the eight subunits of the augmin complex, fly dim γ-tubulin 4 (Dgt4) and human augmin-like complex, subunit 8 (HAUS8)/HICE1 are MT-associated proteins (MAPs) and are likely responsible for establishing the augmin–MT interaction (Wu et al., 2008; Uehara et al., 2009). Because no obvious homologs of NEDD1/GCP-WD or augmin have been found in fungal cells, it is questioned whether they represent an animal cell–specific MT nucleation mechanism.

Functional analysis of proteins like γ-tubulin in animals is often impeded by the lack of stable mutants due to their essential roles in mitosis. In the model plant *Arabidopsis thaliana*, null mutations of essential genes can often be transmitted through heterozygous plants as shown in our previous studies (Lee et al., 2007; Zeng et al., 2009). Haploid mutant microspores produced by heterozygous plants are amenable for phenotypic characterization. In angiosperms, microspores undergo an asymmetrical cell division (pollen mitosis I) to produce a lens-shaped generative cell and a larger vegetative cell. A specialized MT array called the generative pole MT system (GPMS) predicts where the asymmetric mitosis takes place at the cell periphery in orchids (Brown and Lemmon, 1991). The spindle has its peripheral pole anchored at or near the plasma membrane and its interior pole pointing at the center of the microspore (Brown and Lemmon, 1992). Mitotic phenotypes caused by lethal mutations can be analyzed by dissecting defects in MT organization in the spindle and phragmoplast during this asymmetric cell division.

We previously showed that a plant NEDD1-related protein colocalizes with γ-tubulin in the spindle and phragmoplast and is essential for MT organization during mitosis (Zeng et al., 2009). Therefore, we were intrigued to search for possible parallel mechanisms underlying MT nucleation during mitosis in plant cells as seen in animal cells. Putative augmin homologs are indeed found in *Arabidopsis* and rice (*Oryza sativa*). Consistent with the nomenclature of augmin proteins in other systems (Lawo et al., 2009), homologs are named *Arabidopsis AUGMIN* (*AUG*) here. We characterized the role of *Arabidopsis* AUG3 in the assembly of the spindle and phragmoplast MT arrays during male gametogenesis. We propose that an augmin complex is likely formed in plant cells based on the evidence of the in vivo interaction of AUG3 with AUG1. The identification of this complex in plant cells allows us to take a step toward understanding the mechanisms that underlie MT organization during plant cell division.

RESULTS

An Augmin HAUS3 Homolog in *Arabidopsis*

When the amino acid sequences of human augmin subunits (Lawo et al., 2009) were compared with proteins encoded by the *Arabidopsis* genome, it was found that the 617–amino acid AUG3 protein shares noticeable sequence homology to the 478–amino acid C4orf15/HAUS3 (see Supplemental Figure 1 online). AUG3 is relatively acidic with a pI of 5.55. This feature is shared by its human counterpart, which has an isoelectric point of 5.40. Putatively orthologous proteins were identified in rice and moss (*Physcomitrella patens*) with high sequence identity/similarity (see Supplemental Figure 1 and Supplemental Table 1 online). The limited sequence homology between AUG3 and HAUS3 or Dgt3 raised the question of whether it truly functioned as the counterparts in the animal augmin complexes.

At AUG3 Is an Essential Gene

A T-DNA insertional mutation (*aug3-1*) in the 13th exon (Figure 1A) was detected in heterozygous plants that were isolated from a community-generated T-DNA pool (Alonso et al., 2003). When the progeny of a heterozygous +/*aug3-1* plant was analyzed, no homozygous mutants were recovered, indicating that *AUG3* is likely an essential gene. Among the progeny, 38% ($n = 187$) had the +/*aug3-1* genotype, while the remaining 62% were +/+. When the siliques produced by the +/*aug3-1* plant were examined, aborted embryos and unfertilized ovules were frequently observed together with mature seeds (Figure 1B). Compared with the siliques of a wild-type plant, which produced 94% mature seeds and 6% unfertilized ovules, those of +/*aug3-1* had 61% mature seeds, 25% unfertilized ovules, and 14% aborted embryos (sample size = 10 siliques) (Figure 1C). Thus, we believed that the distorted genetic segregation exhibited by the +/*aug3-1* plant was likely due to the combination of gamete sterility and embryo lethality. Based on results of reciprocal crosses between +/*aug3-1* and wild-type plants, it was found that the fertility of both male and female was affected (see Supplemental Table 2 online). The transmission efficiency of the mutation through the male gamete was 60% and that through the female gamete was 37%. Thus, we speculated that AUG3 is an essential protein.

We first examined developing pollen grains to assess the function of AUG3. When the nucleus was stained with the DNA-specific dye 4′,6-diamidino-2-phenylindole (DAPI), almost all pollen grains collected from mature anthers of the wild-type plant had two brightly stained sperm nuclei and one faint vegetative nucleus ($n = 400$; Figure 1D). Among the pollen grains produced by the +/*aug3-1* plant, however, 72% were trinucleate ($n = 404$). In the remaining pollen grains, 11% contained two nuclei of one brightly stained generative nucleus and one faint vegetative nucleus. In addition, 1% pollen grains included only one nucleus and 15% were shrunken in which no discernible nucleus could be visualized by DAPI staining (Figures 1D and 1E). To test whether the phenotype was caused by meiotic defects, we continued to examine the pollen grains produced by +/*aug3-1 qrt*/*qrt* plants. The *qrt*/*qrt* pollen grains failed to separate so that tetrad analysis was made possible (Preuss et al., 1994). The +/*aug3-1 qrt*/*qrt* plant always produced four attached pollen grains, but shrunken pollen grains were often found to be attached to well enlarged ones (red arrows, Figure 1F). Such a phenotype was not observed in pollen produced by the control *qrt*/*qrt* plant. This result suggests that AUG3 is likely required for mitotic cell division as revealed by defects in pollen mitosis caused by the *aug3-1* mutation. Because no homozygous mutant was obtained, it was not tested whether the mutation caused a partial or complete loss of AUG3 function.

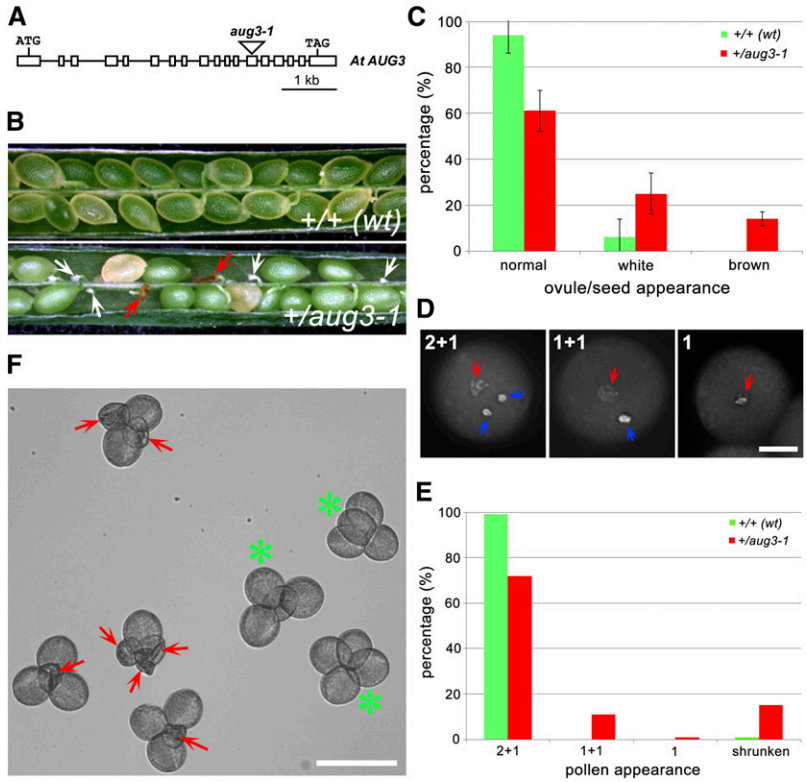

Figure 1. Defects Caused by the *aug3-1* Mutation.

(A) *AUG3* and the *aug3-1* insertional mutation. Exons are shown as open boxes and introns as lines.
(B) The *aug3-1* mutation causes defects in developing fruits/siliques. Compared with the siliques produced by the +/+ (wild type [*wt*]) control plant, those of the heterozygous +/*aug3-1* plant often contain white unfertilized ovules (white arrows) and brown aborted seeds (red arrows).
(C) Scores of normal seeds, unfertilized ovules (white), and aborted seeds (brown) in the control +/+ (wild type) and +/*aug3-1* plants. Error bars represent the standard deviations among examined siliques (n = 10).
(D) Normal and defective pollen grains shown by DNA staining. A normal pollen grain contains two sperm cells with brightly stained nuclei (blue arrows) and a faintly stained vegetative nucleus (red arrow), as classified as the 2+1 type. The defective 1+1 type pollen grain contains a loosely packed vegetative nucleus (red arrow) and a condensed nucleus (blue arrow). The 1 type pollen grain contains only one nucleus containing loosely packed chromatin (red arrow).
(E) Scores of the three types of pollen grains represented in **(D)** and shrunken ones produced by the +/*aug3-1* plant when compared with the wild-type control.
(F) Attached tetrad pollen grains produced by the +/*aug3-1 qrt*/*qrt* plant. Green asterisks indicate the tetrads containing fully enlarged pollen grains. Red arrows point to shrunken pollen grains.
Bars = 5 μm in **(D)** and 50 μm in **(F)**.

We also examined how *aug3-1* affected female gametophyte development and embryogenesis in the ovules produced by the +/*aug3-1 qrt*/*qrt* mutant plants. A wild-type female gametophyte/embryo sac contained an egg cell, two synergids, and a central cell with a conspicuous nucleus (Figure 2A). Defective *aug3-1* embryo sacs were found and had a single enlarged nucleus (Figure 2B). Following pollination, the control ovule produced a proembryo with distinct cell morphology, which was surrounded by cellularized endosperm (Figure 2C). In comparison, the +/*aug3-1* mutant plant produced defective stalk-like embryo structures and did not show obvious cellularization (arrows, Figures 2D and 2E). In addition, a few nuclei were found to float near the defective embryo, indicating that mitotic divisions were blocked during endosperm development (arrowheads, Figure 2E). It was believed that the brownish aborted seeds were derived from ovules containing these defective embryos.

To confirm that the phenotype exhibited by the +/*aug3-1* plant was linked to the T-DNA insertion, +/*aug3-1* mutant plants were transformed with a construct expressing an AUG3-4×c-myc fusion protein driven by its native promoter (see Methods). Among >50 transformants bearing the +/*aug3-1* genotype, two were randomly selected for testing the functionality of the fusion protein and rendered an identical conclusion. In one example, we analyzed genotypes of the progeny of +/*aug3-1* transformed with the *AUG3*-4×c-myc transgene. They gave a ratio of 2.71:1 (n = 193) for *aug3-1* positive (+/*aug3-1*) to negative (+/+) offspring. This result indicated that the distorted segregation ratio of 0.61:1 (38%:62%) was suppressed when AUG3-4xc-myc

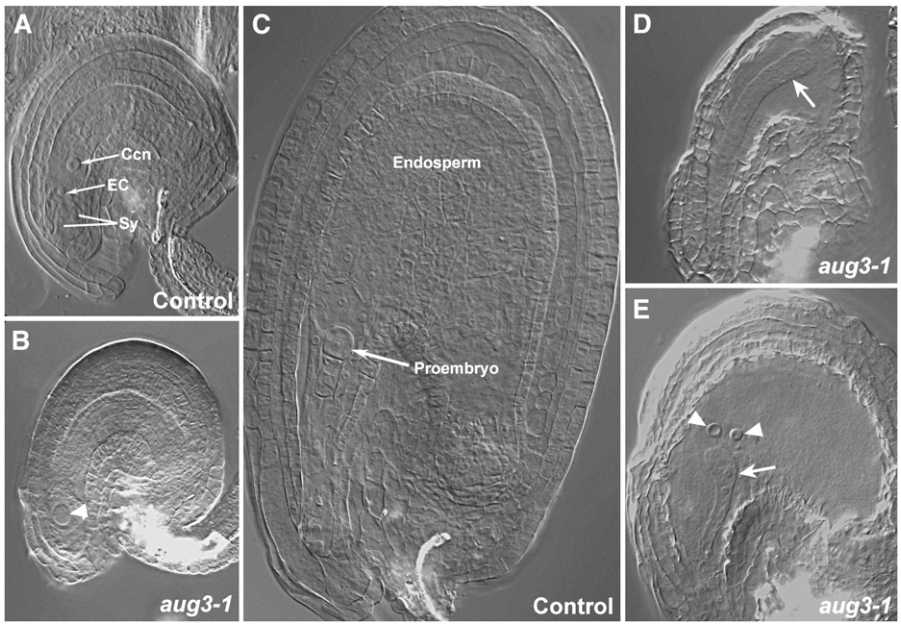

Figure 2. Defects in Ovule Development and Embryogenesis Caused by *aug3-1*.

(A) An ovule produced by a control plant. Inside, an embryo sac contains the egg cell (EC), two synergids (Sy), and a large central cell with a fused nucleus (Ccn).
(B) A defective *aug3-1* embryo sac contains a single abnormally large nucleus (arrowhead).
(C) After fertilization, a proembryo and cellularized endosperm are formed inside the ovule.
(D) and **(E)** Defective embryos (arrows) have not been cellularized, and cells cannot be discerned in areas surrounding the defective embryos. Instead, a few freely suspended nuclei (arrowheads) can be found.

was expressed. We concluded that the above-described defects in gametogenesis and embryogenesis were most likely caused by the inactivation of *AUG3*. It also indicated that the AUG3-4× c-myc fusion was functional.

Abnormal MT Organization in the Spindle and Phragmoplast in the *aug3-1* Mutant

The defects in male gametogenesis caused by the *aug3-1* mutation were further analyzed by comparing MT organization during mitosis in the mutant and wild type control. When the control microspores underwent mitosis (pollen mitosis I), bipolar spindles were assembled toward the periphery of the cell (Figures 3A to 3C). The peripheral half spindle had its wide pole anchored at or near the plasma membrane and the interior half spindle had MTs converged at a single pole pointing to the center of the cell (Figure 3A). Disorganized spindle MTs were observed in mutant cells (Figures 3D to 3L). Abundant MTs connected condensed chromosomes to the cell cortex (Figures 3D and 3G). While the peripheral half spindles contained abundant MT bundles, few MTs were detected in the interior part of the spindle and connected to the chromosomes (arrow, Figure 3I). In these defective pollen grains exhibiting such a half-spindle phenotype, chromosomes were not aligned in the metaphase plate, which could be caused by an imbalanced number of MTs on two sides of the condensed chromosomes. Some developing pollen grains exhibited milder defects in spindle MT organization (Figures 3J to 3L). In the metaphase spindles, the interior half spindle did not have kinetochore fibers that converged to an obvious pole (arrow, Figure 3L). In addition, the spindle clearly crossed the center of the pollen grain and was elongated when compared with the control spindles (Figures 3A and 3J). Such defects were not observed in control pollen grains undergoing mitosis. Among developing pollen grains at metaphase produced by the heterozygous +/*aug3-1* plant ($n = 84$), 39% exhibited the half-spindle phenotype, 14% had defective spindles like that shown in Figure 3J, and the remaining 47% bore normal spindles as seen in the control cells.

At late anaphase and telophase, the control spindles were still restricted to one side of the cell and had MT bundles formed in the midzone (bidirectional arrow, Figures 4A to 4C). In defective cells at similar stages, elongated spindles almost reached the full diameter of the pollen grains and showed rich long bundles in the midzone (bidirectional arrow, Figures 4D to 4F). During cytokinesis in the control cell, MTs reorganized into a curved phragmoplast array by which a curved cell plate would be brought about, as marked by a dark midline in antitubulin immunofluorescence (Figures 4G to 4I). Defective phragmoplasts in the *aug3-1* mutant cells often had loosely packed and disorganized MTs, which appeared between two reforming nuclei (Figures 4J to 4L). Such defective phragmoplasts would result in failed cytokinesis.

Localization of AUG3 in the Spindle and Phragmoplast

Because the AUG3-4×c-myc fusion protein was functional, we used anti-c-myc antibodies to detect the fusion protein in

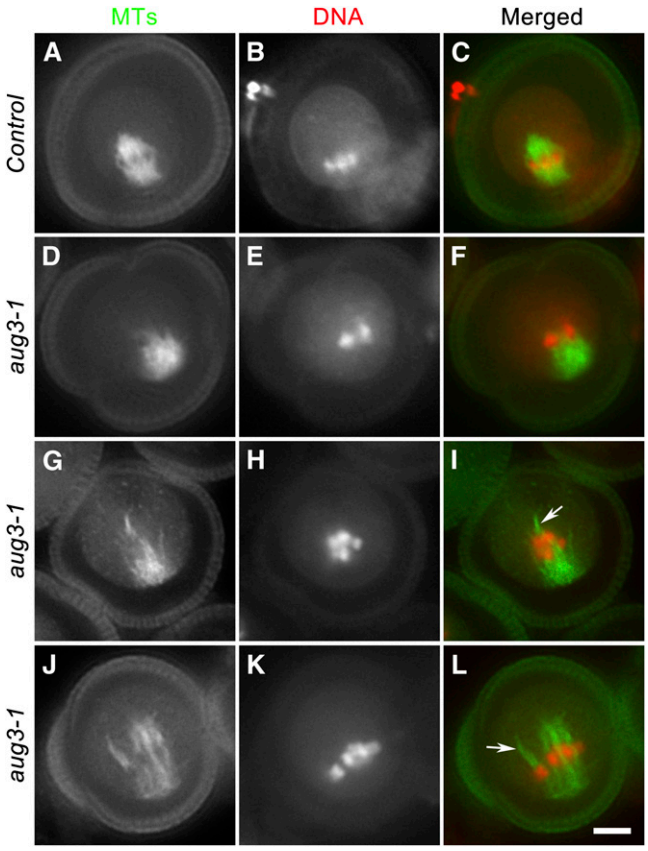

Figure 3. Spindle Defects Caused by the *aug3-1* Mutation.

Spindles of pollen mitosis I are shown for the control (**[A]** to **[C]**) and *aug3-1* (**[D]** to **[L]**) cells. In the merged images, MTs are pseudocolored in green and DNA in red.

(A) to **(C)** A metaphase spindle of the control cell contains converged spindle poles pointing toward the center of the cell. The spindle is placed toward the cell periphery.

(D) to **(F)** MTs formed at the cell periphery and chromosomes are attached to the half spindle.

(G) to **(I)** While the peripheral half spindle contains abundant MTs, only a few MT bundles (arrow) formed in the interior side.

(J) to **(L)** A bipolar spindle contains kinetochore fiber MTs that failed to converge to a common pole (arrow). Bar = 5 μm.

transgenic plants expressing the protein. When root meristematic cells were examined, conspicuous punctate signals were detected in spindles and phragmoplasts (Figure 5). No noticeable signal was detected in wild-type control cells using the identical anti-c-myc antibodies (see Supplemental Figure 2 online). AUG3-4×c-myc was prominent on the prophase nuclear envelope, decorating MTs in the prophase spindle by immunofluorescence (Figures 5A to 5C). In metaphase cells, the punctate anti-AUG3-4xc-myc signal distributed along MTs of kinetochore fiber (Figures 5D to 5F). At anaphase, the AUG3-4xc-myc fusion protein became particularly prominent toward two spindle poles and less signal was detected among midzone MTs between two sets of segregated chromosomes (Figures 5G to 5I). At telophase, when midzone MTs developed into a bipolar phragmoplast MT array as highlighted by a dark antitubulin line in the middle, AUG3-4xc-myc appeared along phragmoplast MTs (Figures 5J to 5L). In cells bearing a mature phragmoplast, punctate AUG3-4xc-myc signal appeared along MTs (Figures 5M to 5O). However, the AUG3-4xc-myc immunofluorescence had a wider dark zone encompassing the developing cell plate compared with that of antitubulin (arrowheads, Figure 5M). The localization pattern suggested a possible bias toward MT minus ends, as shown by anti-γ-tubulin immunofluorescence (Liu et al., 1993).

To further reveal the dynamics of AUG3 in cell division, a functional AUG3-green fluorescent protein (GFP) fusion protein was expressed under the control of its native promoter to resolve

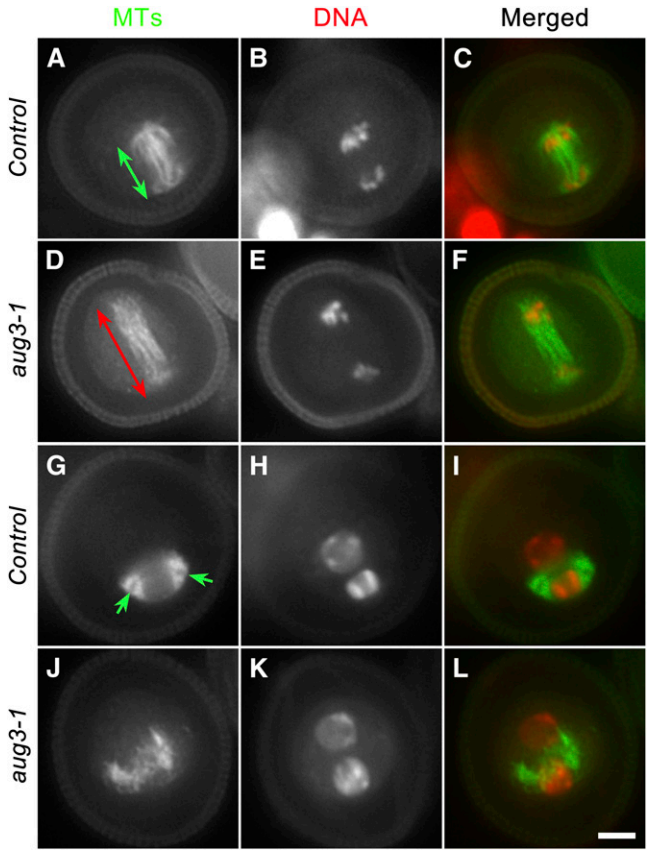

Figure 4. Defects in the Development of the Phragmoplast MT Array Caused by the *aug3-1* Mutation.

MTs in the spindle midzone and phragmoplast are shown in developing pollen grains of the control (**[A]** to **[C]** and **[G]** to **[I]**) and *aug3-1* (**[D]** to **[F]** and **[J]** to **[L]**) mutant. In the merged images, MTs are pseudocolored in green and DNA in red.

(A) to **(C)** Upon completion of anaphase in a control cell, a relatively short spindle (green bidirectional arrow) is placed toward the cell periphery and contains ambient MTs in the spindle midzone.

(D) to **(F)** An *aug3-1* cell exhibits an elongated spindle (red bidirectional arrow), which contains MT bundles in the spindle midzone.

(G) to **(I)** A control cytokinetic cell exhibits a curved phragmoplast with a clear midline (green arrows).

(J) to **(L)** An *aug3-1* cell contains disorganized MTs between two reforming nuclei. Bar = 5 μm.

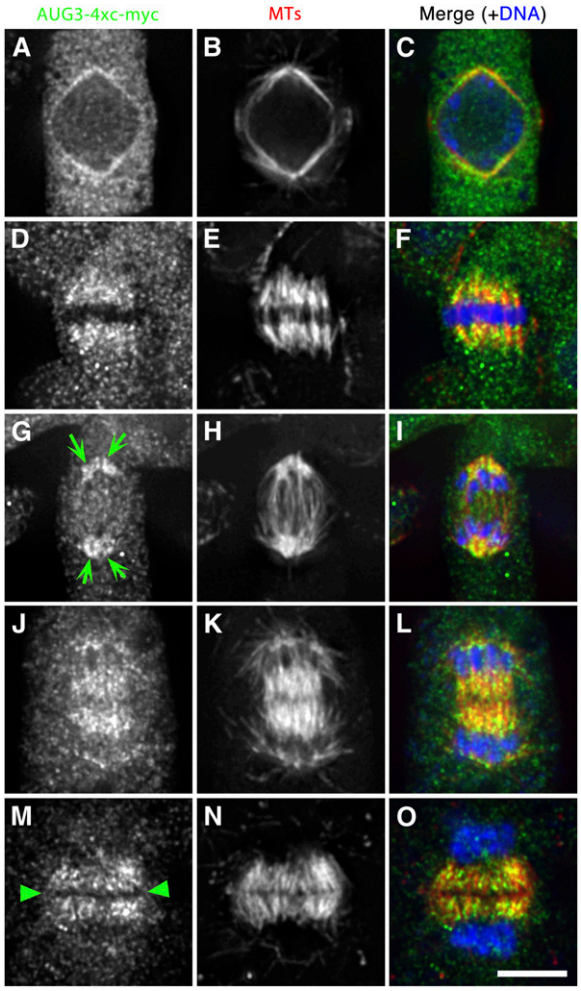

Figure 5. Localization of AUG3 in Mitotic Cells in Root Meristematic Cells.

In merged images, AUG3 is pseudocolored in green, MTs in red, and DNA in blue.

(A) to **(C)** In a prophase cell, the AUG3-4xc-myc signal decorates MTs on the nuclear envelope.

(D) to **(F)** AUG3-4xc-myc appears along kinetochore MT fibers as a punctate signal in a metaphase cell.

(G) to **(I)** During anaphase, AUG3-4xc-myc conspicuously decorates the remnants of kinetochore fibers (green arrows).

(J) to **(L)** At telophase/early cytokinesis, spindle midzone MTs are organized into an antiparallel array. Punctate AUG3-4xc-myc signal can be detected along the MT bundles.

(M) to **(O)** Phragmoplast MTs are decorated with the AUG3-4xc-myc signal. The dark gap in the middle (green arrowheads) left by the AUG3-4xc-myc signal appears to be wider than in the MT fluorescent image. Bar = 5 μm.

its activity in live cells continuously during mitosis. The GFP signal was readily detected in the mitotic spindle at metaphase in a root meristematic cell undergoing mitosis (see Supplemental Movie 1 online; Figure 6A). Conspicuous AUG3-GFP signal was detected at the spindle poles when the cell entered anaphase, especially at later stages of anaphase (arrows, Figures 6B and 6C). At late anaphase and telophase, the GFP signal became noticeable in the spindle midzone, although not as prominent as that at the spindle poles (Figure 6C). While the GFP signal diminished at the spindle poles when the cell progressed toward cytokinesis, it became more striking in the midzone (Figures 6D and 6E). The appearance of AUG3-GFP in the phragmoplast left behind a wide dark region in the center, indicating that AUG3 did not appear at or near the MT plus ends in the phragmoplast midzone (arrowheads, Figure 6E). Instead, AUG3-GFP might have decorated MT minus ends. Dual localization of AUG3-4xc-myc and γ-tubulin by immunofluorescence showed that they both decorated anaphase spindle poles and phragmoplast similarly (see Supplemental Figure 3 online).

The spatial and temporal localization pattern of AUG3-GFP reminded us of that of a GFP fusion of the γ-tubulin complex subunit GCP2 (Nakamura et al., 2010). Indeed, the GCP2-GFP fusion gave a very similar dynamic localization pattern as AUG3-GFP reported in dividing cells (see Supplemental Movie 2 online; Figures 6F to 6J). For example, GCP2-GFP also marked the anaphase spindle poles (arrows, Figure 6H). In addition, the GFP fluorescence left a wide gap in the middle of the phragmoplast, a pattern shown by AUG3-GFP as well (arrowheads, Figure 6J). The comparable localization patterns of AUG3-GFP and GCP2-GFP allowed us to conclude that AUG3 likely colocalized with the γ-tubulin complex in the mitotic spindle and phragmoplast.

AUG3 Is Critical for γ-Tubulin Localization during Mitosis

Because AUG3 and GCP2 exhibited similar localization patterns, we asked whether the localization of γ-tubulin would be altered in the *aug3-1* mutant cells. Using the G9 antibody (Horio et al., 1999), γ-tubulin was detected in the phragmoplast of a dividing microspore (Figures 7A to 7C). The localization of γ-tubulin differed from that of MTs by presenting a wide dark gap in the middle region (arrowheads, Figure 7A). In a developing pollen grain of the *aug3-1* mutant bearing a defective phragmoplast MT array, however, the γ-tubulin signal was no longer concentrated along the MTs (Figures 7D to 7F). Instead, the signal became largely diffuse in the cytosol (Figure 7D). Thus, we concluded that AUG3 is critical for the accumulation of γ-tubulin during mitosis. This result is similar to the finding that the augmin complex plays a role in γ-tubulin localization during mitosis in animal cells (Goshima and Kimura, 2010). Furthermore, we would like to suggest that the disorganized and defective spindle MT arrays exhibited by the *aug3-1* mutant cells were probably the result of altered localization of γ-tubulin in dividing microspores.

AUG1 and AUG3 Are in a Plant Augmin Complex

Besides *AUG3*, *AUG1* encodes a 299–amino acid protein that shares limited sequence identity to the 202–amino acid protein CCDC5/HAUS1 (see Supplemental Figure 4 and Supplemental Table 3 online). AUG1 is an acidic protein with a calculated pI of 5.64. Again, this feature is shared by HAUS1, which has a pI of 5.41. It was suggested that the human CCDC5/HAUS1 protein did not have an obvious homolog in fly and worm (Goshima et al., 2008; Lawo et al., 2009; Uehara et al., 2009). The homology

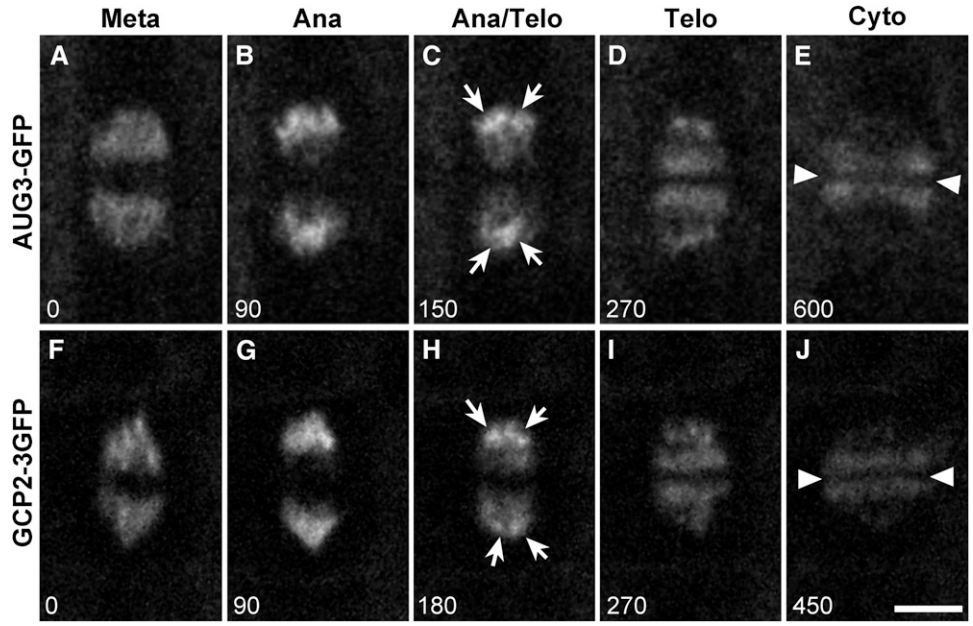

Figure 6. Localization of AUG3 and the γ-Tubulin Complex Protein GCP2 in Live Cells.

Snapshots were taken from time-lapse movies covering metaphase to cytokinesis in root meristematic cells undergoing mitosis. The starting time is set at 0, and individual images are at time (in seconds) after the starting time and are shown on the bottom left.

(A) to **(E)** AUG3-GFP in the spindle and phragmoplast. At metaphase (Meta), the GFP signal appears in the spindle. The signal becomes more prominent at spindle poles during anaphase (Ana). At late anaphase and telophase (Telo), conspicuous AUG3-GFP remains associated with the spindle poles (arrows), while weaker signals can be discerned toward the spindle midzone. The appearance of AUG3-GFP in the phragmoplast leaves a wide gap in the middle region (arrowheads) during cytokinesis (Cyto).

(F) to **(J)** GCP2-GFP gives a similar dynamic localization pattern as AUG3-GFP. Conspicuous signal can be seen at the spindle poles (arrows) during late anaphase and telophase. A wide dark midzone can be detected in the phragmoplast during cytokinesis (arrowheads). Bar = 5 μm.

between AUG1 and HAUS1 prompted us to test whether the AUG1 protein was associated with AUG3 in vivo. To do so, the functional AUG3-4×c-myc fusion protein was enriched from the aforementioned transgenic seedling by an immobilized anti-c-myc antibody (Figure 8). This protein fraction was subject to immunoblotting using anti-c-myc and anti-AUG1 antibodies separately. The AUG3-4×c-myc protein was detected at the position of apparent molecular mass of 78 kD (Figure 8). The anti-AUG1 antibody detected a band at 34 kD (Figure 8), which was consistent with the predicted molecular weight of AUG1. These bands were absent from the fraction derived from the extract of wild-type seedlings, suggesting that they were specific (Figure 8). Furthermore, when the anti-AUG1 antibodies were preabsorbed with the fusion protein used as the antigen, the 34-kD band was no longer detected (Figure 8). This result suggested that the anti-AUG1 antibodies specifically recognized the endogenous AUG1 protein.

If AUG1 and AUG3 were in the same complex, they would exhibit similar localization patterns. We tested AUG1 localization by expressing an AUG1-GFP fusion under the control of its native promoter in stable transgenic lines and imaged its localization over time in a mitotic cell (see Supplemental Movie 3 online). Similarly to what was observed for AUG3-GFP, AUG1-GFP exhibited conspicuous localization at anaphase spindle poles (arrows, Figure 9A). The signal gradually appeared in the midzone (arrows, Figure 9B). Again, its localization in the phragmoplast left a wide gap in the midzone, similar to that presented by the AUG3-GFP and GCP2-GFP fusion (arrowheads, Figure 9C). Thus, the finding that AUG1 and AUG3 have a similar localization pattern supports the notion that AUG1 and AUG3 interact in vivo and are most likely in an augmin-like complex.

DISCUSSION

Our results show that *Arabidopsis* AUG1 and AUG3 occur in an augmin-like complex and decorate the MT arrays of the mitotic spindle and phragmoplast in a pattern similar to that of the γ-tubulin complex protein GCP2. In *Arabidopsis*, augmin plays a critical role in the formation of the spindle and phragmoplast MT arrays. The same can most likely be said for all plants, due to the presence of homologs of AUG1 and AUG3. Thus, an augmin-dependent mechanism underlying MT organization during cell division appears to be evolutionarily conserved among plants and animals.

AUG1 and AUG3 Are Two Subunits of the Augmin Complex in *Arabidopsis*

The animal augmin complex consists of eight subunits (Goshima et al., 2008; Lawo et al., 2009; Uehara et al., 2009). Currently it is

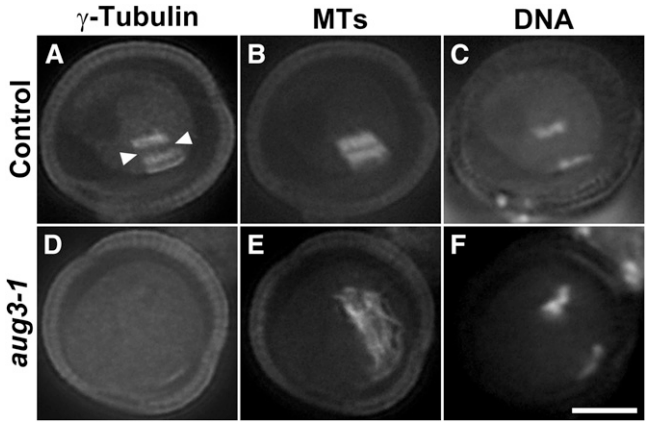

Figure 7. Diminished γ-Tubulin Localization in the Phragmoplast of the *aug3-1* Mutant.

Triple localizations of γ-tubulin, MTs, and DNA in developing microspores of the control (**[A]** to **[C]**) and *aug3-1* (**[D]** to **[F]**) mutant.
(A) to **(C)** In the control cell, conspicuous γ-tubulin signal **(A)** can be detected in the developing phragmoplast. The dark zone in the anti-γ-tubulin fluorescent image (arrowheads) is much wider than that in the MT fluorescent image.
(D) to **(F)** Disorganized MT bundles **(E)** can be detected between two sets of segregated chromosomes **(F)**. γ-Tubulin is not obviously detected among MTs. Bar = 5 μm.

unclear whether the plant augmin complex also contains eight subunits. Based on sequence alignment, a published study presented that significant homology can be found among plant proteins and the animal Dgt3/HAUS3 subunits across the polypeptides (Lawo et al., 2009). The study also revealed plant proteins that share homologies to particular domains of the Dgt5/HAUS5 and Dgt6/HAUS6 subunits. This study identified the AUG1 subunit. Despite limited homology between AUG1 and CCDC5/HAUS1, our localization and in vivo interaction data demonstrate that AUG1 is a subunit of the plant augmin complex. Interestingly, certain augmin subunits, such as Dgt1 and CCDC5/HAUS1 (Lawo et al., 2009; Uehara et al., 2009) and the fly subunit Wac (Meireles et al., 2009), are not well conserved even between fly and mammals. Limited sequence homology prevented us from concluding the presence of homologs of other subunits. Nevertheless, we can conclude that plants also contain a functional augmin complex that interacts with MTs in mitotic arrays. The composition of the plant augmin complex will be resolved upon the purification of the intact complex from plant cells.

Although it is certain now that augmin is present in both animals and plants, it is unclear whether a similar protein complex functions in fungi. It has been shown that in the filamentous fungus *Aspergillus nidulans*, the AN6187 locus encoded a hypothetical protein that shares limited sequence homology to HAUS6 and Dgt6 at their N termini (Lawo et al., 2009). However, it is unclear whether this fungal protein plays any role in MT nucleation in hyphal cells. Fungi do not have proteins that bear obvious sequence homology to Dgt3/HAUS3, CCDC5/HAUS1, or Dgt2. In fission yeast, spindle pole body–independent MT nucleation also takes place in addition to predominant MT nucleation events at the spindle pole body (Sawin and Tran, 2006). However, such events have largely been described in interphase yeast cells and not in the organization of the spindle MT array. Moreover, the proteins involved in these nonessential MT nucleation events discovered in fission yeast were not conserved even among fungal species. It is unclear whether the spindle pole body–independent MT nucleation event in fission yeast resembles features of the centrosome-independent mechanism that requires augmin in plant and animal cells. Whether augmin was lost in fungi during evolution is also an intriguing question. Nevertheless, we propose that such an augmin-dependent and centrosome-independent MT nucleation mechanism must be an ancient one due to its existence in both plants and animals.

Augmin Localization and Function in the Spindle and Phragmoplast

In animal cells, augmin is a MAP complex that likely recruits the γ-tubulin complex to the MT surface via the WD40 repeat protein NEDD1 (Zhu et al., 2008). The localization of γ-tubulin and NEDD1 at the centrosome, however, is independent of augmin (Zhu et al., 2008; Uehara et al., 2009). In plant cells, γ-tubulin is associated with spindle and phragmoplast MTs (Liu et al., 1993, 1994). However, the localization pattern is uneven along MTs. It

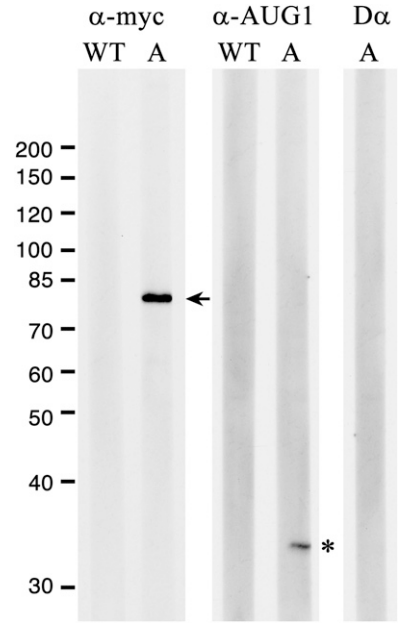

Figure 8. Interaction of AUG3 and AUG1 in Vivo.

Immunoblotting with anti-c-myc (α-myc) and anti-AUG1 (α-AUG1) antibodies. Protein samples were prepared from extracts of wild-type (WT) seedlings and those expressing AUG3-4xc-myc (A). In the negative control, the AUG3-4xc-myc–enriched proteins were probed with an anti-AUG1 depleted preparation (Dα). The AUG3-4xc-myc band is highlighted by an arrow and AUG1 by an asterisk. The AUG band is no longer detected after the specific anti-AUG1 antibodies were depleted. Molecular masses in kilodaltons are shown on the left.

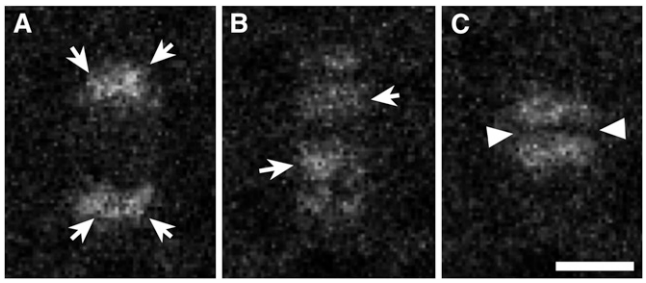

Figure 9. AUG1-GFP in a Root Cell Undergoing Mitosis.

Snapshots of AUG1-GFP at late anaphase to telophase. Conspicuous GFP signal can be seen at spindle poles and in the midzone (arrows). A wide dark zone (arrowheads) can be seen in the middle of the phragmoplast. Bar = 5 μm.

appears in a gradient with the highest concentration toward spindle poles and phragmoplast distal ends facing reforming daughter nuclei (Liu et al., 1995). NEDD1 exhibits an identical localization pattern as γ-tubulin (Zeng et al., 2009). Thus, γ-tubulin appears at the positions where MT minus ends are normally expected. This study showed that *Arabidopsis* AUG1 and AUG3 exhibited a localization pattern similar to that of γ-tubulin, as shown in both the anaphase spindle and the phragmoplast. Furthermore, the *aug3-1* mutant cells showed reduced localization of γ-tubulin in mitotic MT arrays. Both lines of evidence support a function for augmin in mediating the interaction between the γ-tubulin complex and spindle and phragmoplast MTs.

At late anaphase and telophase, AUG1/3-GFP fusions quickly appeared at the spindle midzone in live cells. The disorganized phragmoplast MT array exhibited by the *aug3-1* cells suggested that plant augmin also plays a role in the organization of phragmoplast MTs, probably via the amplification of MTs. We would like to suggest that the accumulation of augmin along spindle midzone MTs may be critical for the recruitment of γ-tubulin to produce a functional phragmoplast MT array. This assumption is consistent with the recent findings on the role of augmin in generating new MTs in the spindle midzone in animal cells (Goshima and Kimura, 2010; Uehara and Goshima, 2010).

In human cells, augmin interacts with MTs via the HICE1/HAUS8 subunit, which is a MAP (Wu et al., 2008; Uehara et al., 2009). Similarly, the fly augmin subunit Msd1 also functions as a MAP (Wainman et al., 2009). However, no obvious homologs of either NICE1/HAUS8 or Msd1 could be identified in plants based on the primary amino acid sequences. If the mechanism of augmin–MT interaction is conserved in animals and plants, a MAP is also expected to occur in the plant complex. Isolation of a sufficient amount of the plant augmin complex is key to discovering this missing MAP.

Published studies on augmin focused on its role in MT amplification and organization in spindles. A GFP fusion of the human HAUS4 subunit can be detected at the centrosome in interphase cells (Uehara et al., 2009). However, the augmin complex was copurified with the γ-tubulin ring complex from mitotic cells but not interphase cells (Teixidó-Travesa et al., 2010). This is somewhat surprising, because γ-tubulin is also abundant at the centrosome during interphase (Zheng et al., 1991). It suggests that augmin interacts with the γ-tubulin ring complex, possibly in a cell cycle–dependent manner. In plant cells, γ-tubulin appears along cortical MTs (Liu et al., 1995). However, we could not detect γ-tubulin in augmin-enriched preparation by immunoblotting. In cells expressing AUG1/3-GFP, the fluorescent signal was so weak that even the signal inside the spindle was quickly bleached during image acquisition with a spinning disk confocal microscope. Hence, whether augmin interacts with cortical MTs is still an open question.

Augmin-Dependent and -Independent MT Organization during Spindle Formation

In orchids, when the microspore undergoes mitosis, MTs are nucleated at a localized cortical region, namely, the generative pole, toward which the generative cell will be born (Brown and Lemmon, 1991). The GPMS MTs connect the plasma membrane with the nuclear envelope and predict the asymmetrical cell division in the microspore (Brown and Lemmon, 1991). Because this asymmetrical cell division leads to the formation of the generative cell and is ubiquitously found among angiosperms, one would predict that GPMS would be established in microspores of other flowering plants as well. However, recent studies did not detect a similar MT array in tobacco (*Nicotiana tabacum*) and *Arabidopsis* microspores when GFP-tubulin was expressed under the control of a microspore-specific promoter (Oh et al., 2010a, 2010b). Instead, a basket-like MT array was observed on the nuclear envelope that was believed to be responsible for the eccentric nuclear positioning and subsequent asymmetrical cell division (Oh et al., 2010b). Thus, the GPMS may not be a universal feature of pollen mitosis I in angiosperms. This study suggests that there are two pathways that lead to the formation of the peripheral and interior half spindles. In control cells, MT densities in the peripheral and interior half spindles did not show obvious differences upon nuclear envelope breakdown. In *aug3-1* mutant cells, however, the significantly lower MT density in the interior half spindle suggested that augmin was likely required for the formation of new MTs in that region. MTs in the interior half spindle may be amplified from those of the peripheral half spindle anchored at the plasma membrane. Although the mutant microspore did not experience obvious problems in generating sufficient MTs in the peripheral half spindle, later MT amplification based on these MTs might have been significantly hampered. Thus, an imbalanced spindle was born. The phenotype suggests that an augmin-independent MT organization mechanism may be responsible for establishing the MT array of the peripheral half spindle with its pole anchored at or near the plasma membrane. An augmin-dependent mechanism becomes critical for the later stages of MT organization during spindle formation. However, we cannot rule out the possibility that long-living augmin proteins might have been inherited from the heterozygous microsporocyte to function in the formation of the peripheral half-spindle.

Among the defective microspores undergoing mitosis, those that failed to form bipolar spindles most likely were blocked in prometaphase and resulted in shrunken pollen grains. It is

intriguing that some defective cells formed bipolar spindles despite being abnormal. They were formed either via an augmin-independent mechanism or using augmin inherited from the heterozygous microsporocyte. These defective spindles were no longer placed at the cell periphery. Instead, elongated spindles were formed, which might be due to more rigorous MT polymerization in the peripheral half spindle than in the interior one. If so, the chromosomes would be pushed toward the interior part of the cytoplasm. This may have contributed to the conversion of asymmetrical cell division into a more or less symmetrical division in the mutant microspores. It is noteworthy that similar elongated spindles were also observed in *nedd1* mutant cells (Zeng et al., 2009).

Published studies have shown that kinetochore fibers consist of core and skew MTs, giving them the appearance of fir trees, which are readily observed in large dividing cells of the *Haemanthus* endosperm and onion (*Allium cepa*) root meristem (Palevitz, 1988; Smirnova and Bajer, 1992). Skew MTs seem to be branches from the core that may be attached to the kinetochores. It is unclear how these skew MTs contribute to spindle operation. It would not be surprising if their formation were dependent on the functions of γ-tubulin and augmin. If so, we could conclude that the appearance of fir trees might be a critical feature for the dynamic spindle to function in mitosis.

We also observed that augmin was critical for MT formation in the spindle midzone during anaphase. During anaphase and telophase, MTs rapidly polymerize and coalesce in the spindle midzone between two groups of segregating chromatids (Zhang et al., 1990). If augmin functions to recruit γ-tubulin, the loss of such a recruitment role would likely be responsible for the failure of MT formation and organization in the spindle midzone in the *aug3-1* mutant cells. Consequently, the bipolar phragmoplast MT array could not be established because MTs in the spindle midzone give rise to the early form of this array.

When TMBP200, a conserved MAP215/Dis1 family protein in tobacco, was depleted by the microspore-targeted RNA interference, multipolar spindles and fragmented phragmoplasts were formed during pollen mitosis I (Oh et al., 2010b). A published study suggests that the fly augmin subunit Dgt6 interacts with the XMAP215 homolog Msps (Bucciarelli et al., 2009). However, the phenotypes of MT organization caused by the *aug3-1* mutation are different from those caused by knocking down the expression of TMBP200 in dividing microspores (Oh et al., 2010b). In *Arabidopsis*, the *mor1-1* mutation alleles of the putatively orthologous *MOR1/GEM1* also cause similar defects in spindle and phragmoplast MT organization in somatic cells, leading to cell division failures (Twell et al., 2002; Eleftheriou et al., 2005; Kawamura et al., 2006). The allelic *gem1-1* mutation causes cytokinetic defects in dividing microspores, presumably due to disorganized MTs resulting from the lack of functional MOR1/GEM1 (Twell et al., 2002). MOR1/GEM1 and TMBP200 decorate MTs throughout the cell cycle (Twell et al., 2002; Hamada et al., 2004; Kawamura et al., 2006). This family of MAP proteins is known to promote MT polymerization at MT plus ends (Brouhard et al., 2008). However, augmin probably functions specifically in amplifying a sufficient number of MTs by increasing MT nucleation events to produce functional spindle and phragmoplast MT arrays.

METHODS

Plant Materials and cDNA Clones

The *Arabidopsis thaliana* lines used in this study are control Columbia-0 and the SALK_099174 mutant line made available to us by the ABRC at Ohio State University. Full-length *AUG3* and *AUG1* cDNA clones were generated by the *Arabidopsis* research community (Seki et al., 1998, 2002; Castelli et al., 2004). Plant growth conditions and transformation procedures were as described previously (Kong et al., 2010).

Detection/Genotyping of the *aug3-1* Mutation and Phenotypic Characterization

The T-DNA insertion at the *AUG3* locus was detected by PCR using the primers At5g1RP2, 5′-GCTGTCACGGTCATCTACTGCTCCTTGTTC-3′, and LBa1, 5′-TGGTTCACGTAGTGGGCCATCG-3′. The wild-type *AUG3* allele was detected by At5g1RP2 and At5g1LP2, 5′-GGAACAAGTGAGAGACAATGGATTGAAGCC-3′. Back crosses with wild-type plants were performed to confirm that the observed phenotypes were linked to the T-DNA insertion.

Methods used in phenotypic characterization of the defects brought about by the *aug3-1* mutation were as described previously (Zeng et al., 2009). Pollen grains were collected from mature anthers of open flowers. To determine the terminal phenotype of the embryo sac, ovules were dissected from pistils 48 h after emasculation of the flowers. Defects in male gametogenesis were detected by DNA staining using DAPI and those in female gametogenesis and embryogenesis by differential interference contrast microscopy after clearing.

Genetic Suppression/Complementation of the *aug3* Mutation

A 5.9-kb genomic *AUG3* fragment containing the promoter region and the coding sequence was amplified by PCR using the primers 48520-F, 5′-CACCTTTCGTTAAAATGTTCAATATTTTAACAAAAACAAAAATG-3′, and 48520-R, 5′-TGCGCCTGCGCCCGATGATGAGGCTTGGCGAGCACGAAC-3′, and Phusion DNA polymerase (New England Biolabs). Amplified DNA was cloned into the Gateway pENTR/D-TOPO vector (Life Technologies) according to the manufacturer's instructions. The resulting plasmid was recombined with the pGWB16 vector (Nakagawa et al., 2007) by an LR recombination reaction (Life Technologies). Consequently, the pGWB16-*AUG3* plasmid was used for *Agrobacterium tumefaciens*–mediated transformation into the heterozygous +/*aug3-1* mutant. The pGWB16 plasmid contained the 4xc-myc tag-coding sequence to allow a target protein to be tagged at the C terminus. Therefore, transformants would express the AUG3-4×c-myc fusion protein at a level similar to that of the native AUG3 protein.

Segregation patterns of T-DNA insertions were determined by PCR-based genotyping as described above using progeny derived from an untransformed heterozygous mutant and two independent transformants.

Expression of AUG1/3-GFP in *Arabidopsis*

The aforementioned *AUG3* genomic fragment was cloned into the destination vector pGWB4 (Nakagawa et al., 2007) by recombination to give rise to pGWB4-AUG3, which was used for transformation. A 2.4-kb fragment of AUG1 was amplified from a genomic DNA preparation by PCR using the primers 41350-F, 5′-CACCTTTTGAAATTT TTTGCTTCACATTTTATAC-3′, and 41350-R, 5′-TGCGCCTGCGCCCTCATCGTTTGTCTCAAGGGCTGATTG-3′. After being cloned into pENTR/D-TOPO, this fragment was then inserted into pGWB4 to yield the pGWB4-AUG1 plasmid, which was used for transformation.

Generation of Anti-AUG1 Antibodies

The coding region of AUG1 was amplified using the U21622 plasmid as template by the primers U21622F, 5′-ATATGGATCCCCATGGGTATG-AGCGACGTC-3′, and U21622R, 5′-ATCGGAGCTCTCACTCATCGTT-TGT-3′, and Pfx DNA polymerase (Life Technologies). The resulting fragment was cloned into the pGEX-KG vector at the *Nco*I and *Sac*I sites after the fragment and vector were digested by these enzymes. The recombinant plasmids rendered the expression of GST-AUG1 fusion protein in bacteria host BL21 (DE3) (Life Technologies). The fusion protein was purified using immobilized glutathione (Thermo Scientific) according to the manufacturer's instructions and used as the antigen for immunization of mice. Antibody production and purification were as described previously (Kong et al., 2010).

Determination of AUG3–AUG1 Interaction in Vivo

Proteins were extracted from control *Arabidopsis* plants and transformants expressing the AUG3-4×c-myc fusion. Briefly, 3-d-old etiolated seedlings were frozen in liquid nitrogen and ground to powder using a mortar and pestle. An extraction buffer of 50 mM Tris HCl, pH 8.0, containing 150 mM NaCl and 1% Triton X-100 was added to the powder. The supernatant was collected after centrifugation at 15,000*g* and filtration through a 0.45-μm Millex HV filter (Millipore). The AUG3-4×c-myc fusion protein was enriched by anti-c-myc antibody-conjugated magnetic beads according to the manufacturer's instructions (Miltenyi Biotec).

Proteins enriched for the c-myc–tagged proteins from *Arabidopsis* seedlings were separated on a 7.5% SDS-PAGE gel before being transferred to polyvinylidene fluoride membranes (Millipore) for immunoblotting. The AUG3-4×c-myc fusion was detected by the 9E10 anti-c-myc antibody (Developmental Studies Hybridoma Bank at University of Iowa) and native AUG1 by the antibodies described above. To confirm that the band detected by the anti-AUG1 antibodies was indeed the protein encoded by At2g41350, the antibodies were preabsorbed by the GST-AUG1 fusion protein prior to immunoblotting.

Immunolocalization and Fluorescence Microscopy

Immunolocalization of tubulins in pollen grains was performed as described previously (Lee et al., 2007). The AUG3-4×c-myc fusion protein was detected by rabbit anti-c-myc antibodies (Sigma-Aldrich) in root tip cells of transgenic lines using protocols described previously (Lee et al., 2001). MTs were labeled by sheep antitubulin antibodies (Cytoskeleton). Images were acquired with a CFI Plan Fluor ×100 objective (numerical aperture of 1.3) under an Eclipse 600 epifluorescence microscope (Nikon) or a UPlan Apo ×100 (numerical aperture of 1.35; Olympus) under a DeltaVision microscope (Applied Precision).

To observe AUG1/AUG3/GCP2-GFP signals, seeds were germinated on agar medium containing half-strength Murashige and Skoog salt. Seedlings were observed under a Marianas spinning disk confocal microscope (Intelligent Imaging Innovations) using a Plan-Apo ×63 objective (Carl Zeiss). Samples expressing GFP fusions were illuminated at 488 nm by a diode-pumped solid-state laser, and the standard enhanced GFP setting was used for GFP capturing by an EMCCD camera driven by the Slidebook 5.0 software.

Figures and movies presented here were assembled in the Metamorph (Molecular Devices) or SoftWoRx (Applied Precision) software packages.

Accession Numbers

The At *AUG1* and At *AUG3* genes were identified by The Arabidopsis Information Resource as At2g41350 and At5g48520, and their cDNA clones used in this study had the GenBank accession numbers of BX832241 and U21622, respectively.

Supplemental Data

The following materials are available in the online version of this article.

Supplemental Figure 1. Alignment of the AUG3/HAUS3/Dgt3 Sequences.

Supplemental Figure 2. Negative Control of Anti-c-myc Immunolocalization.

Supplemental Figure 3. Dual Localizations of AUG3 and γ-Tubulin.

Supplemental Figure 4. Alignment of the AUG1 and HAUS1 Sequences.

Supplemental Table 1. Amino Acid Sequence Identity and Similarity among At AUG3, Os AUG3, Pp AUG3, HAUS3, and Dgt3.

Supplemental Table 2. Transmission Efficiency of the *aug3-1* Mutation.

Supplemental Table 3. Amino Acid Sequence Identity and Similarity among At AUG1, Os AUG1, Pp AUG1, and HAUS1.

Supplemental Movie 1. AUG3-GFP, Pseudocolored in Green, in a Dividing Root Cell.

Supplemental Movie 2. GCP2-GFP, Pseudocolored in Green, in a Dividing Root Cell.

Supplemental Movie 3. AUG1-GFP, Pseudocolored in Green, in a Dividing Root Cell.

ACKNOWLEDGMENTS

We thank the ABRC (Ohio State University), Hélène Bergès (Centre National de Ressources Genomiques Vegetales of Institut National de la Recherche Agronomique, France), Masayoshi Nakamura (Nara Institute of Science and Technology), Takashi Hashimoto (Nara Institute of Science and Technology), and Tetsuya Horio (University of Kansas) for providing the T-DNA insertion lines, cDNA clones, the GCP2-GFP line, and the G9 antibody. This report is based on work supported by the National Science Foundation under Grant MCB-0920454 and by the U.S. Department of Energy under Contract DE-FG02-04ER15554. Any opinions, findings, and conclusions or recommendations expressed in this report are those of the authors and do not necessarily reflect the views of the National Science Foundation or the Department of Energy.

AUTHOR CONTRIBUTIONS

B.L. designed the project. C.-M.K.H, T.H., Z.K., Y.-R.J.L., J.S., and C.J.T.Z. performed specific experiments and analyzed data. C.-M.K.H, T.H., Z.K., Y.-R.J.L., C.J.T.Z., and B.L. wrote the article together. Y.-R.J.L. and B.L. revised and edited the manuscript.

Received April 28, 2011; revised June 12, 2011; accepted June 28, 2011; published July 12, 2011.

REFERENCES

Alonso, J.M., et al. (2003). Genome-wide insertional mutagenesis of *Arabidopsis thaliana*. Science **301:** 653–657.

Ambrose, J.C., and Cyr, R. (2008). Mitotic spindle organization by the preprophase band. Mol. Plant **1:** 950–960.

Brouhard, G.J., Stear, J.H., Noetzel, T.L., Al-Bassam, J., Kinoshita,

K., Harrison, S.C., Howard, J., and Hyman, A.A. (2008). XMAP215 is a processive microtubule polymerase. Cell **132:** 79–88.

Brown, R.C., and Lemmon, B.E. (1991). Pollen development in orchids 3. A novel generative pole microtubular system predicts unequal pollen mitosis. J. Cell Sci. **99:** 273–281.

Brown, R.C., and Lemmon, B.E. (1992). Pollen development in orchids 4. Cytoskeleton and ultrastructure of the unequal pollen mitosis in phalaenopsis. Protoplasma **167:** 183–192.

Bucciarelli, E., Pellacani, C., Naim, V., Palena, A., Gatti, M., and Somma, M.P. (2009). Drosophila Dgt6 interacts with Ndc80, Msps/XMAP215, and γ-tubulin to promote kinetochore-driven MT formation. Curr. Biol. **19:** 1839–1845.

Castelli, V., et al. (2004). Whole genome sequence comparisons and "full-length" cDNA sequences: a combined approach to evaluate and improve Arabidopsis genome annotation. Genome Res. **14:** 406–413.

Eleftheriou, E.P., Baskin, T.I., and Hepler, P.K. (2005). Aberrant cell plate formation in the *Arabidopsis thaliana microtubule organization 1* mutant. Plant Cell Physiol. **46:** 671–675.

Goshima, G., and Kimura, A. (2010). New look inside the spindle: Microtubule-dependent microtubule generation within the spindle. Curr. Opin. Cell Biol. **22:** 44–49.

Goshima, G., Mayer, M., Zhang, N., Stuurman, N., and Vale, R.D. (2008). Augmin: A protein complex required for centrosome-independent microtubule generation within the spindle. J. Cell Biol. **181:** 421–429.

Goshima, G., Wollman, R., Goodwin, S.S., Zhang, N., Scholey, J.M., Vale, R.D., and Stuurman, N. (2007). Genes required for mitotic spindle assembly in Drosophila S2 cells. Science **316:** 417–421.

Hamada, T., Igarashi, H., Itoh, T.J., Shimmen, T., and Sonobe, S. (2004). Characterization of a 200 kDa microtubule-associated protein of tobacco BY-2 cells, a member of the XMAP215/MOR1 family. Plant Cell Physiol. **45:** 1233–1242.

Horio, T., Basaki, A., Takeoka, A., and Yamato, M. (1999). Lethal level overexpression of γ-tubulin in fission yeast causes mitotic arrest. Cell Motil. Cytoskeleton **44:** 284–295.

Hutchins, J.R.A., et al. (2010). Systematic analysis of human protein complexes identifies chromosome segregation proteins. Science **328:** 593–599.

Job, D., Valiron, O., and Oakley, B. (2003). Microtubule nucleation. Curr. Opin. Cell Biol. **15:** 111–117.

Karsenti, E., and Vernos, I. (2001). The mitotic spindle: A self-made machine. Science **294:** 543–547.

Kawamura, E., Himmelspach, R., Rashbrooke, M.C., Whittington, A.T., Gale, K.R., Collings, D.A., and Wasteneys, G.O. (2006). MICROTUBULE ORGANIZATION 1 regulates structure and function of microtubule arrays during mitosis and cytokinesis in the Arabidopsis root. Plant Physiol. **140:** 102–114.

Kong, Z., Hotta, T., Lee, Y.R., Horio, T., and Liu, B. (2010). The γ-tubulin complex protein GCP4 is required for organizing functional microtubule arrays in *Arabidopsis thaliana*. Plant Cell **22:** 191–204.

Lawo, S., et al. (2009). HAUS, the 8-subunit human Augmin complex, regulates centrosome and spindle integrity. Curr. Biol. **19:** 816–826.

Lee, Y.-R.J., Giang, H.M., and Liu, B. (2001). A novel plant kinesin-related protein specifically associates with the phragmoplast organelles. Plant Cell **13:** 2427–2439.

Lee, Y.R.J., Li, Y., and Liu, B. (2007). Two *Arabidopsis* phragmoplast-associated kinesins play a critical role in cytokinesis during male gametogenesis. Plant Cell **19:** 2595–2605.

Liu, B., Joshi, H.C., and Palevitz, B.A. (1995). Experimental manipulation of γ-tubulin distribution in Arabidopsis using anti-microtubule drugs. Cell Motil. Cytoskeleton **31:** 113–129.

Liu, B., Marc, J., Joshi, H.C., and Palevitz, B.A. (1993). A γ-tubulin-related protein associated with the microtubule arrays of higher plants in a cell cycle-dependent manner. J. Cell Sci. **104:** 1217–1228.

Liu, B., Joshi, H.C., Wilson, T.J., Silflow, C.D., Palevitz, B.A., and Snustad, D.P. (1994). γ-Tubulin in *Arabidopsis*: Gene sequence, immunoblot, and immunofluorescence studies. Plant Cell **6:** 303–314.

Lloyd, C., and Chan, J. (2006). Not so divided: The common basis of plant and animal cell division. Nat. Rev. Mol. Cell Biol. **7:** 147–152.

Lüders, J., and Stearns, T. (2007). Microtubule-organizing centres: A re-evaluation. Nat. Rev. Mol. Cell Biol. **8:** 161–167.

Meireles, A.M., Fisher, K.H., Colombié, N., Wakefield, J.G., and Ohkura, H. (2009). Wac: A new Augmin subunit required for chromosome alignment but not for acentrosomal microtubule assembly in female meiosis. J. Cell Biol. **184:** 777–784.

Murata, T., Sonobe, S., Baskin, T.I., Hyodo, S., Hasezawa, S., Nagata, T., Horio, T., and Hasebe, M. (2005). Microtubule-dependent microtubule nucleation based on recruitment of γ-tubulin in higher plants. Nat. Cell Biol. **7:** 961–968.

Murata, T., Tanahashi, T., Nishiyama, T., Yamaguchi, K., and Hasebe, M. (2007). How do plants organize microtubules without a centrosome? J. Integr. Plant Biol. **49:** 1154–1163.

Nakagawa, T., Kurose, T., Hino, T., Tanaka, K., Kawamukai, M., Niwa, Y., Toyooka, K., Matsuoka, K., Jinbo, T., and Kimura, T. (2007). Development of series of gateway binary vectors, pGWBs, for realizing efficient construction of fusion genes for plant transformation. J. Biosci. Bioeng. **104:** 34–41.

Nakamura, M., Ehrhardt, D.W., and Hashimoto, T. (2010). Microtubule and katanin-dependent dynamics of microtubule nucleation complexes in the acentrosomal Arabidopsis cortical array. Nat. Cell Biol. **12:** 1064–1070.

Nakamura, M., and Hashimoto, T. (2009). A mutation in the Arabidopsis γ-tubulin-containing complex causes helical growth and abnormal microtubule branching. J. Cell Sci. **122:** 2208–2217.

Oh, S.A., Allen, T., and Twell, D. (2010a). A ticket for the live show: Microtubules in male gametophyte development. Plant Signal. Behav. **5:** 614–617.

Oh, S.A., Pal, M.D., Park, S.K., Johnson, J.A., and Twell, D. (2010b). The tobacco MAP215/Dis1-family protein TMBP200 is required for the functional organization of microtubule arrays during male germline establishment. J. Exp. Bot. **61:** 969–981.

Palevitz, B.A. (1988). Microtubular fir-trees in mitotic spindles of onion roots. Protoplasma **142:** 74–78.

Palevitz, B.A. (1993). Morphological plasticity of the mitotic apparatus in plants and its developmental consequences. Plant Cell **5:** 1001–1009.

Preuss, D., Rhee, S.Y., and Davis, R.W. (1994). Tetrad analysis possible in Arabidopsis with mutation of the *QUARTET* (*QRT*) genes. Science **264:** 1458–1460.

Sawin, K.E., and Tran, P.T. (2006). Cytoplasmic microtubule organization in fission yeast. Yeast **23:** 1001–1014.

Seki, M., Carninci, P., Nishiyama, Y., Hayashizaki, Y., and Shinozaki, K. (1998). High-efficiency cloning of Arabidopsis full-length cDNA by biotinylated CAP trapper. Plant J. **15:** 707–720.

Seki, M., et al. (2002). Functional annotation of a full-length Arabidopsis cDNA collection. Science **296:** 141–145.

Smirnova, E.A., and Bajer, A.S. (1992). Spindle poles in higher plant mitosis. Cell Motil. Cytoskeleton **23:** 1–7.

Teixidó-Travesa, N., Villén, J., Lacasa, C., Bertran, M.T., Archinti, M., Gygi, S.P., Caelles, C., Roig, J., and Lüders, J. (2010). The gammaTuRC revisited: A comparative analysis of interphase and mitotic human gammaTuRC redefines the set of core components and identifies the novel subunit GCP8. Mol. Biol. Cell **21:** 3963–3972.

Twell, D., Park, S.K., Hawkins, T.J., Schubert, D., Schmidt, R., Smertenko, A., and Hussey, P.J. (2002). MOR1/GEM1 has an essential role in the plant-specific cytokinetic phragmoplast. Nat. Cell Biol. **4:** 711–714.

Uehara, R., and Goshima, G. (2010). Functional central spindle assembly requires de novo microtubule generation in the interchromosomal region during anaphase. J. Cell Biol. **191:** 259–267.

Uehara, R., Nozawa, R.S., Tomioka, A., Petry, S., Vale, R.D., Obuse, C., and Goshima, G. (2009). The augmin complex plays a critical role in spindle microtubule generation for mitotic progression and cytokinesis in human cells. Proc. Natl. Acad. Sci. USA **106:** 6998–7003.

Wainman, A., Buster, D.W., Duncan, T., Metz, J., Ma, A., Sharp, D., and Wakefield, J.G. (2009). A new Augmin subunit, Msd1, demonstrates the importance of mitotic spindle-templated microtubule nucleation in the absence of functioning centrosomes. Genes Dev. **23:** 1876–1881.

Wiese, C., and Zheng, Y. (2006). Microtubule nucleation: γ-Tubulin and beyond. J. Cell Sci. **119:** 4143–4153.

Wu, G., Lin, Y.T., Wei, R., Chen, Y., Shan, Z., and Lee, W.H. (2008). Hice1, a novel microtubule-associated protein required for maintenance of spindle integrity and chromosomal stability in human cells. Mol. Cell. Biol. **28:** 3652–3662.

Zeng, C.J., Lee, Y.R., and Liu, B. (2009). The WD40 repeat protein NEDD1 functions in microtubule organization during cell division in *Arabidopsis thaliana*. Plant Cell **21:** 1129–1140.

Zhang, D.H., Wadsworth, P., and Hepler, P.K. (1990). Microtubule dynamics in living dividing plant cells: Confocal imaging of microinjected fluorescent brain tubulin. Proc. Natl. Acad. Sci. USA **87:** 8820–8824.

Zheng, Y.X., Jung, M.K., and Oakley, B.R. (1991). γ-Tubulin is present in *Drosophila melanogaster* and *Homo sapiens* and is associated with the centrosome. Cell **65:** 817–823.

Zhu, H., Coppinger, J.A., Jang, C.Y., Yates III, J.R., and Fang, G. (2008). FAM29A promotes microtubule amplification via recruitment of the NEDD1-γ-tubulin complex to the mitotic spindle. J. Cell Biol. **183:** 835–848.